UPPSALA
UNIVERSITET

The role of RNA-binding protein FUBL-1 in epigenetic inheritance in C. elegans

Nouha Abdelaziz

Degree project in biology, Master of science (2 years), 2022
Examensarbete i biologi 45 hp till masterexamen, 2022
Biology Education Centre and Department of Cell and Molecular Biology , Uppsala University
Supervisor: Andrea Hinas

Table of Contents

Abstract

Gene silencing by RNA interference is conserved, systemic and heritable in *Caenorhabditis elegans.* This phenomenon is crucial to protect *Caenorhabditis elegans* from pathogens and non-self-invaders. Furthermore, this defence mechanism is not restricted to the parents and can be epigenetically passed to the progeny RNA interference pathways. RNA interference pathways in *Caenorhabditis elegans* are divided into exogenous and endogenous depending on small RNA origin. In both pathways, primary small RNAs trigger secondary 22 nucleotide long small RNAs with 5' Guanosine bias (22G) synthesis and amplification, which in turn promotes gene expression reduction referred to as ''silencing''. However, the mechanism of epigenetic inheritance through RNA interference is still not understood. In this study, I investigated the role of an RNA-binding protein, FUBL-1 in RNA interference endogenous pathway in *Caenorhabditis elegans.* I showed that there was no statistically significant difference between *fubl-1 Δ* and *fubl-1 iso a (-)* in ERGO1 target gene *E01G4.5* (n=2, p-value: 0.07). The nonsense mutation affecting all predicted isoforms (*fubl-1 isoform a+c (-))* showed a similar upregulation as deletion as expected. The findings suggest that FUBL-1a might have a crucial role downstream in the 26G pathway and might bind to 22G transported to the nucleus as it has a nuclear localisation signal. Furthermore, RT-qPCR results showed a similar expression of both tested ERGO-1 target genes in wild type and *fubl-1*::3xFLAG (p-value: 0,596 for *E01G4.5*, *p-value:* 0,845 for *E01G4.7*) indicating that the FLAG tag does not affect FUBL-1 function. Immunoprecipitation pilot experiment was successfully performed, and results suggest that FUBL-1 binds to mRNA and might interact with small RNAs.

List of abbreviations

DNA	deoxyribonucleic acid
RNA	ribonucleic acid
C. elegans	*Caenorhabditis elegans*
lncRNAS	long non-coding ribonucleic acids
RNAi	ribonucleic acid interference
L1, L2, L3, L4	larval stage 1, 2, 3, 4
piRNAs	PIWI-interacting ribonucleic acids
miRNAs	micro-ribonucleic acids
siRNA	small interfering ribonucleic acids
AGO	argonaute
RISC	ribonucleic acid induced silencing complex
RdRP	RNA-dependent RNA polymerase
dsRNA	double stranded ribonucleic acids
RBP	RNA-binding protein
FUBL-1	far-upstream element binding protein like-1
KH domain	K homology domain
NLS	nuclear localization signal
DUF	domain of unknown function
RT-qPCR	reverse transcription quantitative polymerase chain reaction
RNA-IP	ribonucleic acid immunoprecipitation
E. coli	*Escherichia coli*
cDNA	complementary deoxyribonucleic acid
KCl	potassium chloride
KOH	potassium hydroxide
kDa	kilodalton
bp	base pair
SDS PAGE	sodium dodecyl sulfate polyacrylamide gel electrophoresis
PVDF	polyvinylidene difluoride membrane
TBS-T	tris buffered saline - tween
Hrp	horseradish peroxidase
IP	immunoprecipitation

Introduction

For a long time, the parental influence on offspring's life was believed to be dependent only on genes, and taught culture (Kappeler & Meaney 2010). Unfortunate events such as famine have unveiled a new player in the inheritance game. Accumulated evidence from different famines in Sweden, Netherlands, and China has shown a correlation between the environment, nutrition, parents, and offspring's health that maybe be affected by epigenetics (Heijmans *et al.* 2008; Vågerö *et al.* 2018; Shen *et al.* 2019)

''Epigenetics is the study of heritable changes in gene expression that occur independently of changes in the primary DNA sequence'' (Lacal & Ventura 2018). Epigenetic modification includes DNA methylation, posttranslational histone modification, and effect on gene expression by non-coding RNAs (Lacal & Ventura 2018). Non-coding RNAs are further divided into long non-coding RNAs (lncRNAs) and small non-coding RNAs (Lacal & Ventura 2018).

In this study, I will focus on the regulation of gene expression by RNA interference (RNAi), a small non-coding RNA-mediated sequence specific gene silencing, in *Caenorhabditis elegans* (*C. elegans*) (Fire *et al.*, 1998).

C. elegans is an ideal model to study epigenetic inheritance as RNAi is efficiently passed to progeny (Corsi *et al.* 2015). In addition, *C. elegans* has a 3-day generation time from embryo to adult stage, a sequenced genome, is non-pathogenic, is a hermaphroditic (self-fertilizing) species (although with rare males) and can be synchronized by isolating newly hatched larva or treating gravid adults (adults with one row of embryos) with bleach which disintegrates the adults but does not damage the eggs (Corsi *et al.* 2015).

Figure 1 shows the *C. elegans* lifecycle from embryos to old adult. *C. elegans* has four larval stages after hatching before developing into an egg laying adult hermaphrodite. In case of stress, like starvation, the worm enters an arrest stage known as dauer in which it can survive without food for months (Corsi *et al.* 2015).

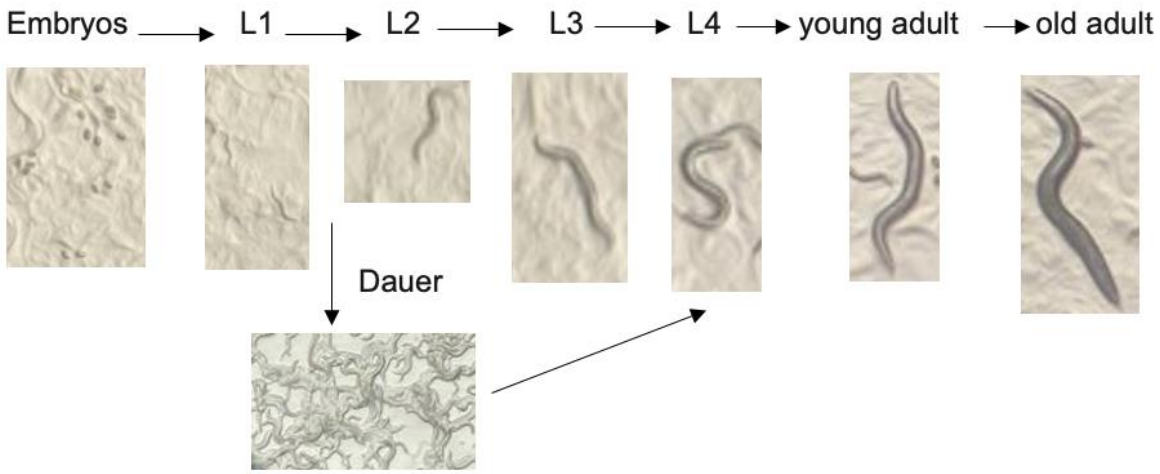

Figure 1: *C. elegans* lifecycle illustration

In metazoa, small RNAs are divided in three classes: PIWI-interacting RNAs (piRNAs), microRNAs (miRNAs), and small interfering RNAs (siRNAs) (Grishok 2005).
Small RNAs bind and guide Argonaute (AGO) protein to target RNA by base pairing forming RNA induced silencing complex (RISC), leading to gene expression reduction either at transcriptional or post-transcriptional level (Grishok 2005).

The RNAi phenomenon mediated by small RNAs was first discovered in *C. elegans* (Fire *et al.*, 1998). RNAi pathways in *C. elegans* are divided into exogenous and endogenous depending on small RNA origin. In both pathways, primary small RNAs trigger secondary 22 nucleotide long small RNAs with 5' Guanosine bias (22G) synthesis and amplification, which in turn promotes gene expression reduction referred to as ''silencing'' (Almeida, Andrade-Navarro and Ketting, 2019).

The exogenous RNAi pathway depends on double stranded RNA (dsRNA) acquisition from the environment. dsRNA is processed into primary siRNA by Dicer enzyme and trigger 22G siRNA by RdRP (Almeida, Andrade-Navarro and Ketting, 2019). Endogenous RNAi pathway include 21U and 26G pathways. Small RNAs in endogenous 26G pathway are produced by mature ERI complex and is divided in two different subpopulations responsible for gene silencing through 22G production: the ALG 3/4 in the male germline and L4 spermatogenic hermaphrodite and the ERGO-1 oocytic/embryonic in L1, L2 hermaphrodite and embryos (Almeida, Andrade-Navarro and Ketting, 2019). The latter is of interest for the current study.

Figure 2 illustrates the proposed endogenous oocytic/embryonic 26G RNAi biogenesis pathway. 26G small RNAs are produced by mature ERI complex and processed by HENN-1. ERGO-1 bound 26G small RNA guide it to its target mRNA to promote 22G small RNA synthesis. Next, RNA-dependent RNA polymerase (RdRP) is recruited to amplify 22G small RNAs synthesis and trigger gene silencing. Gene silencing is promoted through histone tail modifications or transcription pausing on transcriptional level or through mRNA degradation or stalling ribosomes on post-transcriptional level (Almeida, Andrade-Navarro and Ketting, 2019). Gene regulation through small RNA pathways is intricate as a deficiency in one pathway may promote silencing through another pathway (Almeida, Andrade-Navarro and Ketting, 2019).

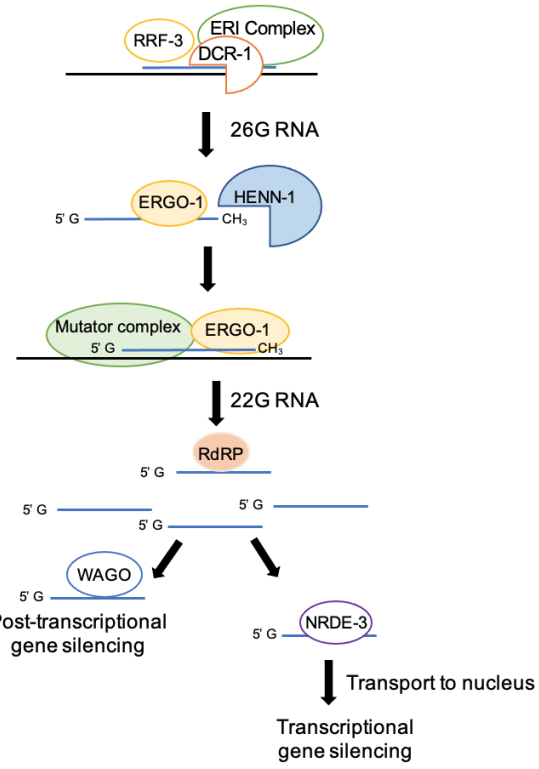

Figure 2: Oocytic/embryonic 26G RNA biogenesis Pathway (modified from (Almeida, Andrade-Navarro and Ketting, 2019))

26G RNAs are produced by ERI complex including RRF-3 and DCR-1, and 2'-O-methylated by HENN-1. ERGO-1 bound 26G RNA guide ERGO-1 to its target mRNA to trigger 22G synthesis. 22G are produced by RdRP and are responsible for gene silencing on transcriptional or post-transcriptional level. (RdRP: RNA dependent RNA Polymerase)

RNA-binding proteins (RBPs) are crucial to regulate mRNA lifecycle including splicing, transport, and stability (Theil *et al.* 2019). *C. elegans* Far upstream element binding protein like-1 (FUBL-1) encodes a putative RBP, orthologue of human Far upstream element binding proteins, which are involved in transcriptional and post-transcriptional regulation in mammals (WormBase website)

Kim and colleagues (2005) previously conducted a genome wide RNAi screen in epidermal seam cells in *C. elegans*, reporting that *fubl-1* knockdown perturbs dsRNA mediated gene silencing. Other studies showed that FUBL-1 interacts with various proteins, including proteins involved in pre-mRNA processing and chromatin modifications/remodeling as well as post-transcriptional regulation (Li *et al.*, 2004, Wu *et al.*, 2017). However, FUBL-1 function has not been further investigated.

FUBL-1 has four K homology (KH) domains, and a conserved C-terminal domain of unknown function (DUF). The *fubl-1* gene has three predicted coding sequences isoform a, b1/b2, and c (WormBase website). *fubl-1* isoform c is part of isoform a and isoform a but not c has a predicted nuclear localization signal (Figure 3).

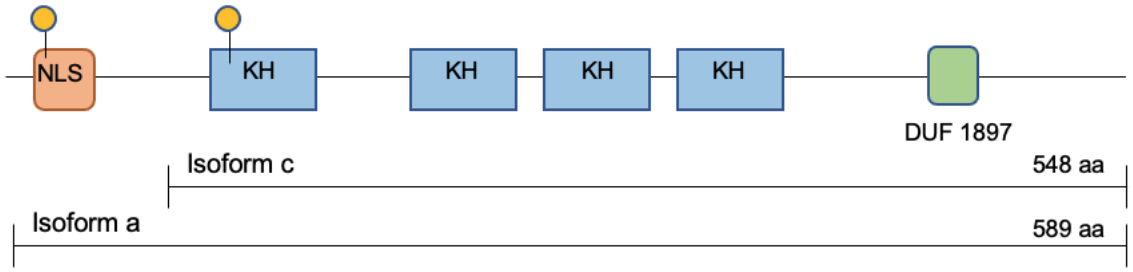

Figure 3: *fubl-1* isoform A and C (NLS: nuclear localization signal, DUF: domain of unknown function)

The Hinas group has examined the subcellular localization of FUBL-1 using FUBL-1::mCherry fusion protein construct (Roy et al., manuscript in preparation). The construct showed expression in different cell types and localized in the cytoplasm, nucleus, perinuclear foci, and embryos (Roy et al., manuscript in preparation). This experiment could not differentiate if different subcellular localization represents different FUBL-1 isoforms, or the result of phosphorylation, as the mCherry fusion tag was added to the C-terminus of FUBL-1 sequence. In addition, the role of different isoforms in RNAi is still not understood.

The host laboratory (Hinas group at ICM) has investigated the role of FUBL-1 in exogenous RNAi pathway in *C. elegans.* Strains lacking a functional *fubl-1* gene have a stronger exogenous RNAi response (Roy et al., manuscript in preparation). This is probably because it acts in oocytic/embryonic 26G RNA pathway which has been shown to compete with exogenous RNAi pathway (Almeida, Andrade-Navarro and Ketting, 2019). In line with this, mRNAs normally targeted by 26G RNAs are upregulated in a *fubl-1Δ* mutant (Roy et al., manuscript in preparation).

Aims of the study

In this study, the role of *fubl-1* isoforms in ERGO-1 26G endogenous RNAi pathway and how it is involved in gene expression regulation will be investigated.

Aims

1. Investigate whether disrupting *fubl-1* isoform a gives the same phenotype as disruption of all possible isoforms at once using (RT)-qPCR.
2. Investigate if the 3X FLAG tag affects the function of FUBL-1
3. Set up RNA immunoprecipitation (IP) using *fubl-1*::3xFLAG strain

Materials and methods

Worm maintenance

N2 Bristol (wild type) (Brenner, 1974), AHS205 *fubl-1*::3X FLAG six times outcrossed, AHS158 (tm2769)V four times outcrossed (*fubl-1* Δ), AHS170 (gk660081)V (*fubl-1 iso a (-)*), and AHS171 (gk668481)V (*fubl-1 iso a+c (-)*) strains were obtained from Hinas lab. All worms were grown on nematode growth medium (NGM) agar plates seeded with E. coli OP50 (Brenner, 1974) strain unless otherwise mentioned.
E. coli NA22 strain on enriched peptone plates (Evans, 2006) was used to grow worms for protein extraction.

Bleach synchronization

Worms were cultured at 20 ºC. The mixed stages population was collected in M9 buffer and pelleted by centrifugation at 450 x g. Worms were washed with M9 3-4 times to remove bacteria. A solution containing 0.8% sodium hypochlorite and o.5 M KOH was added to the pelleted worms to disrupt worm bodies for 4 min, M9 was added to stop the reaction, and samples were quickly centrifuged. For additional clean up, the pellet was resuspended in 60% sucrose solution and sterile water and centrifuged at 450 x g for 6 min in a swing bucket rotor. Floating eggs were collected in a new tube, centrifuged, resuspended in M9 and eggs were distributed on NGM without bacteria or 8P plates seeded with NA22 (Evans, 2006).

RNA extraction

Worm plates grown for approximately 44 hours after hatching were washed with M9, collected as gravid adults in a 15 ml tube, and centrifuged at 2,400 rpm for 2 min at room temperature. Next, worms were frozen in liquid nitrogen and ground with a micro pestle. After grinding worm pellets, 900 µl TRIzol reagent was added, and worms were ground and vortexed for a few more seconds worm body disruption was checked under microscope. Next, 200 µl chloroform was added, lysates were vortexed and incubated for 10 min at room temperature, then centrifuged at 13,000 rpm at 4 ºC for 15 min. The aqueous phase was removed and transferred to a new tube, followed by a second chloroform extraction. After transferring aqueous phase to a new tube, an equal volume of isopropanol was added, following by mixing, and incubation at room temperature for 10 min. After centrifugation at 13,000 rpm at 4 ºC for 10 min, the pellet was washed with 1.5 ml ice cold 75% ethanol. The

ethanol was removed, and the pellet was left to air dry for 5 min then dissolved in 40 µl sterile water and incubated at 60 ºC for 5 min.

Analysis of RNA quantity and quality

RNA concentration was measured with Nanodrop UV spectrophotometer and RNA integrity was assessed by agarose gels electrophoresis.

cDNA synthesis and RT- qPCR

2 µg of total RNA was treated with DNase I (Thermo Fisher Scientific) by incubation for 30 min at 37 ºC, followed by 5 mM EDTA treatment and DNase I heat inactivation for 10 min at 65 ºC and incubation on ice for 5 min. Then 1 µg of DNase I treated RNA was used to synthesize cDNA with RevertAid H minus Reverse Transcriptase (Thermo Fisher Scientific) according to manufacturer's protocol.

qPCR was performed on StepOnePlus system (BioRad) using 2X SYBR green dye. Reactions were 20 µl total volume (using 2 µl cDNA, 2X SYBR GREEN, 0.1 µM Forward primer, 0.1 µM Reverse primer). Primer sequences listed in table S1. *Eif-3-c* was used as endogenous reference. Three technical replicates were performed for each sample.

Statistical analysis of RT-qPCR data

For each qPCR reaction, ΔCt= (average Ct (gene of interest of each biological replicate) – average Ct (*eif-3-c* of each biological replicate)), normalisation to wild type *eif-3-c* ΔΔCt= (ΔCt – ΔCt (average wild type *eif-3-c*)), fold change and standard deviation were calculated (Yuan *et al.* 2006). One way ANOVA was used for statistical analysis.

***fubl-1*::3xFLAG genotyping**

Worms were collected with 10 mM Tris-HCl (pH 8.3). 1.2 µg/ml proteinase K was added, worms were frozen at -80 ºC for 1 hour and then thawed on ice. The worms were incubated at 65 ºC for 1 hour, followed by proteinase K inactivation at 95 ºC for 15 minutes.

Next, genotyping was performed using worm lysates as template, and a positive control with FLAG flanking sequence specific primers (Primer sequences in table S1). The total reaction volume was 25 µl (using 2.5 µl lysate, 0.2 µM *fubl-1*::3xFLAG forward primer, 0.2 µM *fubl-1*::3xFLAG reverse primer, 10X DreamTaq Green Buffer, 5U/µl DreamTaq polymerase, 10

mM dNTP), with the following PCR conditions (58 ºC annealing for 40 seconds and 72 ºC extension for 35 seconds for 35 cycles and 5 min final extension at 72 ºC).

Protein extraction

Synchronized *C. elegans* were grown on peptone rich 8P agar plates seeded with NA22 (Evans, 2006), and harvested as gravid adults (1 day post L4 stage). The pellet was frozen in liquid nitrogen in aluminum foil and stored at -80 ºC until use.

The frozen pellet was ground in a pre-cooled mortar and pestle and kept cool all the time by addition of liquid nitrogen. After grinding to a fine powder, 400 µl of extraction buffer (50 mM Hepes/KOH pH 7.4, 150 mM KCl, 5mM MgCl2, 10% glycerol, 0.1% (v/v) Triton-X 100, 7 mg/ml protease inhibitor (Thermo Fisher), and 200 U/ml RNase inhibitor (Thermo Fisher)) was added, kept on ice to thaw, and mixed frequently. The lysate was transferred to a pre-chilled Eppendorf tube and cell debris was pelleted at 14,000 rpm for 30 minutes. Next, the supernatant was transferred to a new pre-chilled Eppendorf tube and stored at -80 ºC until further use. Protein concentration was quantified with Bradford assay.

Western blot

Protein lysates were prepared with Laemmli buffer, boiled for 5 minutes at 95 ºC then placed on ice.

Proteins were resolved by SDS-PAGE on precast "any KD Mini-protean Stain-Free'' gels and transferred to PVDF membrane with "Trans-Blot Turbo Mini PVDF Transfer Packs". The membrane was blocked with 3% BSA in TBS-T (50 mM Tris, 150 mM NaCl, 0.05% Tween, pH 7.4 – 7.6) overnight at 4 ºC on a shaker and washed with TBS-T the next day. The membrane was incubated for 1 h at room temperature with "mouse monoclonal ANTI-FLAG M2 Peroxidase (HRP) antibody" (Catalog Number A8592, Sigma) diluted 1:10 000 in TBS-T 3% BSA. The membrane was washed with TBS-T 6 x 5 min and visualized by addition of HRP substrate "Amersham ECL Prime Western Blotting Detection Reagent (Cytivia)'' according to the manufacturer's instruction.

Immunoprecipitation (IP)

Synchronized gravid adults grown on 8P agar seeded with NA22 were lysed in extraction buffer as described in the protein extraction section. Protein concentration was quantified by Bradford assay and 3 mg for protein and 3 mg for RNA elution was aliquoted for each strain.

For each IP 30 µl anti-FLAG M2 magnetic beads (Sigma–Aldrich; M8823) were equilibrated with extraction buffer (without protease and RNase inhibitor), followed by anti-FLAG IP incubation with lysate (corresponding to 3 mg protein) for 3 h at 4 °C on a rotating wheel. Beads were washed 5 x 5 min with extraction buffer (without protease and RNase inhibitor). For RNA-IP, bound RNA was eluted by adding Tri Reagent to the beads. RNA extraction was performed as described above with the eluted RNA and the input sample for each strain. RNA concentration was measured for input sample only due to low amount of RNA in IP and reverse transcription was performed. qPCR analysis was done by calculating for each mRNA ΔCT= CT (IP) - CT (input), relative enrichment (re) re = Δ, and fold enrichment = .
Protein was eluted by incubating the beads with Laemmli buffer (no 2-ME) for 5 min at 70 °C on a shaker. 50 µg protein input and 10% IP eluate for each strain was used for SDS PAGE and Western blot analysis. For total protein detection, the protein gel was incubated with staining solution (0.1% Coomassie R-250 in 40% ethanol and 10% acetic acid) for 1 h at room temperature on a shaker, rinsed with water twice and incubated with de-staining solution (10% ethanol and 7.5% acetic acid) overnight at 4 °C on a shaker.
Western blot was performed as described in western blot section

Results

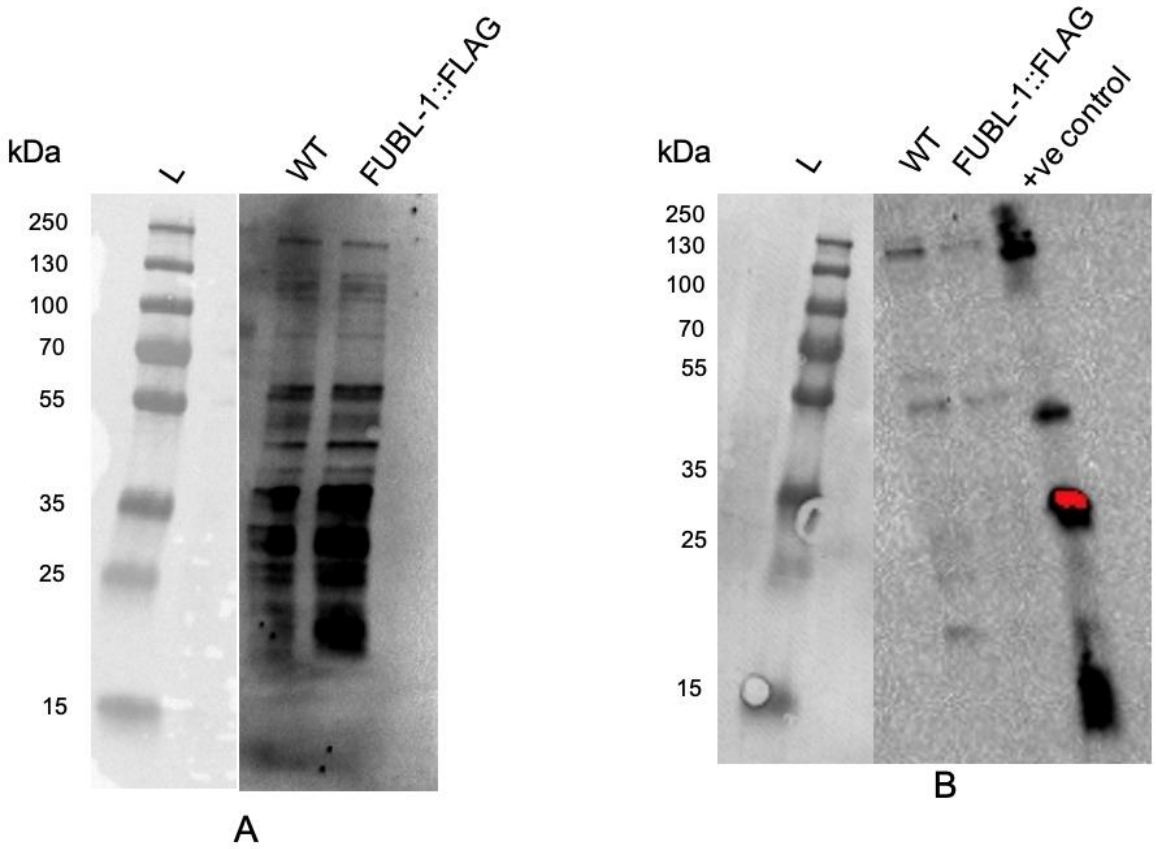

Figure 1: Investigating 3X FLAG tagged FUBL-1 protein expression

(A) Western blot using HRP-conjugated anti-FLAG monoclonal antibody (L: Ladder, WT: wild type total protein, FUBL-1::3xFLAG: *fubl-1*::3xFLAG total protein).

(B) Western blot using HRP-conjugated anti-FLAG monoclonal antibody (L: Ladder, WT: wild type total protein, FUBL-1::3xFLAG: *fubl-1*::3xFLAG total protein, +ve control: FLAG tagged total protein preparation from E. coli expressing another protein)

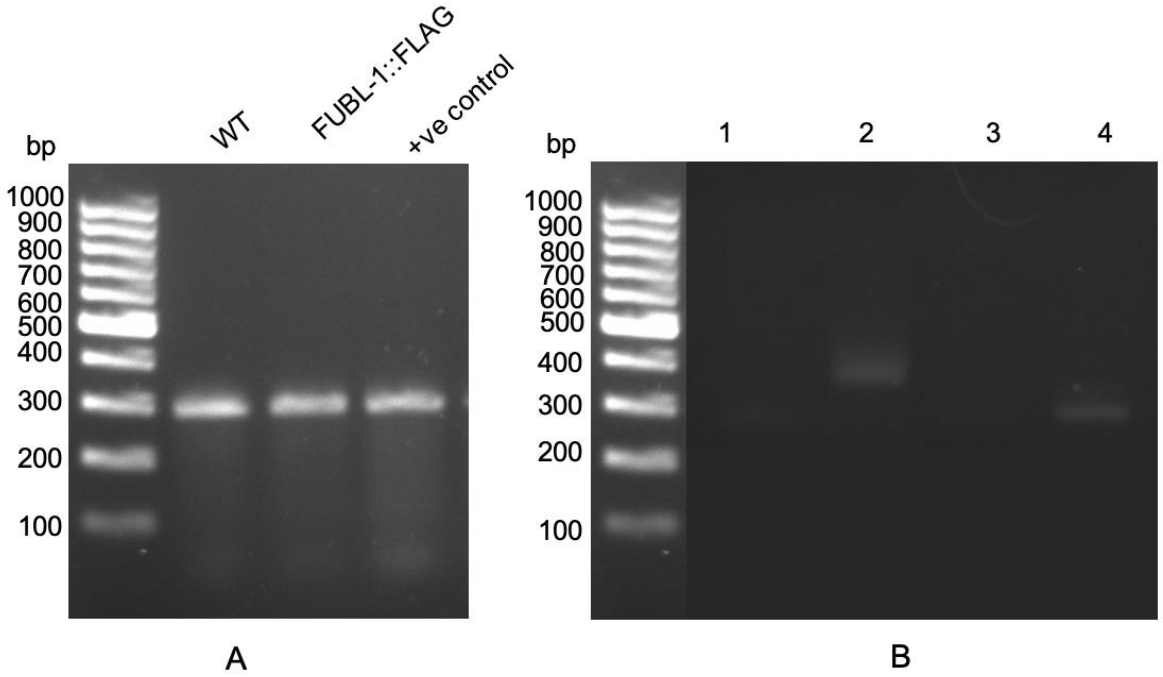

Figure 2: Genotyping wild type and FUBL-1::3xFLAG strains

(A) Genotyping wild type and *fubl-1*::3xFLAG using worm lysates as template (WT: wild type, FUBL-1::FLAG: *fubl-1*::3xFLAG, +ve control: wild type lysate prepared by another group member used as positive control)

(B) 1: fresh Wild type lysate, 2: Fresh *fubl-1*::3xFLAG lysate, 3: old wild type lysate, 4: old *fubl-1*::3xFLAG lysate

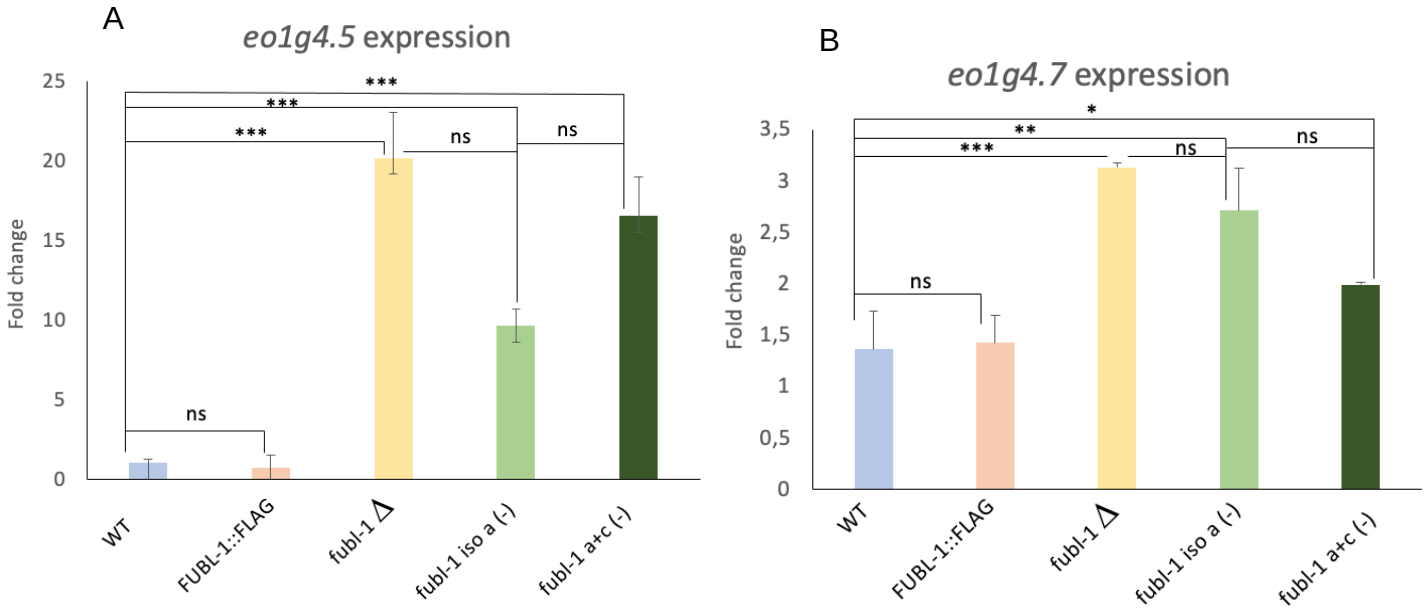

Figure 3: fubl-1 isoform a disruption shows a similar phenotype to all isoforms' disruption

(A) Relative mRNA expression of E01G4.5.

(B) Relative mRNA expression of E01G4.7 in five different strains.

Relative expression was analysed by RT-qPCR in 1 day post L4 in WT, *fubl-1*::3xFLAG, *fubl-1 Δ*, *fubl-1 iso a (-)*, and *fubl-1 iso a+c (-)* (normalized by eif3c) , n=4 for WT, n=3 for *fubl-1*::3xFLAG and *fubl-1 iso a+c (-)*, n=2 for *fubl-1 Δ*, *fubl-1 iso a (-)*,*$p=<0.05$, **$p<0.01$, ***$p<0.001$ by one way ANOVA test.

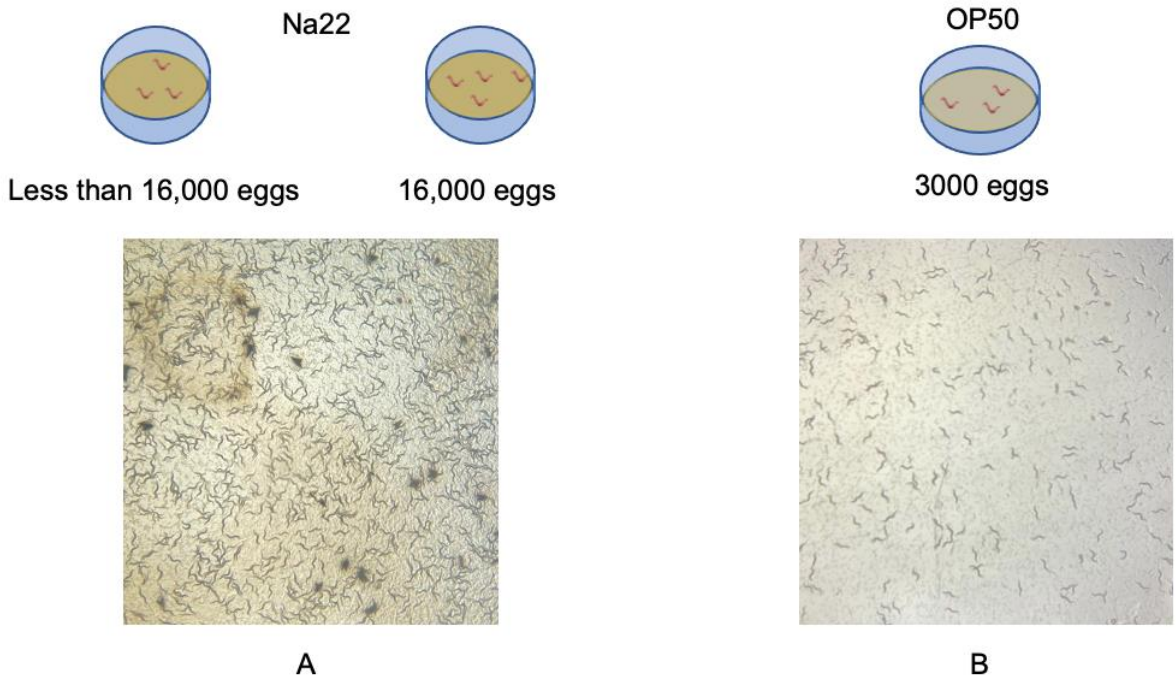

Figure 4: Optimization of C. elegans growth using E. coli strain NA22

(A) around 16000 synchronized gravid adults on peptone rich media seeded with *E. coli* NA22 strain.

(B) around 3000 synchronized gravid adults on NGM media seeded with *E. coli* OP50 strain.

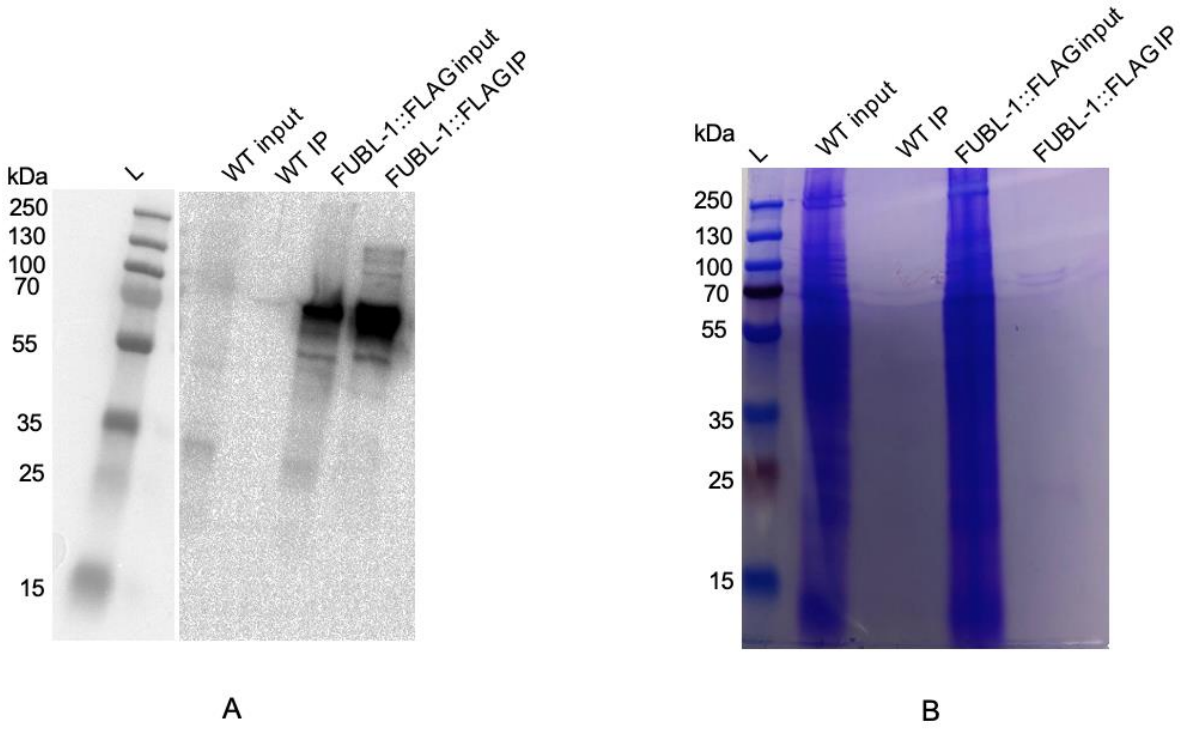

Figure 5: FUBL-1::3xFLAG immunoprecipitation
50 µg input and 10% eluate IP was loaded for each strain for western blot and SDS-PAGE.

(A) Western blot of WT: wild type and FUBL-1::FLAG input and IP eluate.

(B) SDS PAGE of WT: wild type and FUBL-1::FLAG input and IP eluate

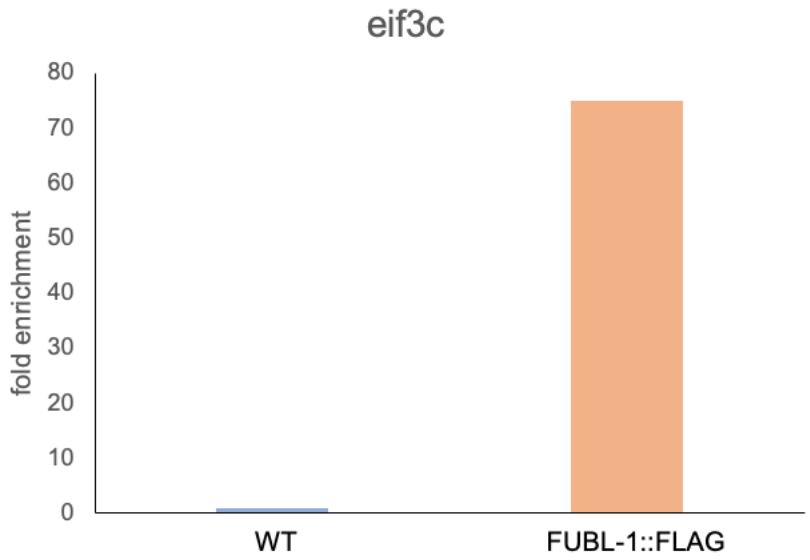

Figure 6: FUBL-1::3xFLAG bound mRNA was successfully eluted
Fold enrichment of eif3c mRNA. Relative expression was analysed by RT-qPCR in 1 day post L4 in pulled down and input WT: wild type and FUBL-1::FLAG (n=1).

Investigating 3X FLAG tagged FUBL-1 protein expression

The Hinas lab has recently constructed a 3X FLAG tagged FUBL-1 strain outcrossed 6 times but has not investigated its expression or whether the FLAG tag affects FUBL-1 function. First, FUBL-1::3xFLAG protein expression was investigated by western blot using total protein lysate of FUBL-1::3xFLAG strain in comparison to wild type (Figure 1(A). The expected size of FLAG-tagged FUBL-1 was around 58-62 kDa (FUBL-1 protein size: FUBL-1 isoform a (62.8 kDa) and FUBL-1 isoform c (58.1 kDa) however there were no visible bands at 70 kDa in FUBL-1::FLAG well. In addition, wild type and FUBL-1::3xFLAG had similar bands, indicating non-specific binding. The results suggested two explanations; either the FUBL-1::3xFLAG strain was mixed with a strain a lacking the FLAG tag or the antibody was not specific for the FLAG. To test the latter, Western blot was repeated with total protein lysates of wild type and FUBL-1::3xFLAG strains, and a FLAG-tagged total protein preparation from an E. coli strain expressing another protein, gifted by Thomas Stenum, was used as a positive control.

In addition, blocking time was increased from 1 to 16 h and antibody staining time was reduced from 16 to 1 h to decrease nonspecific binding. After chemiluminescence detection, bands were observed for the positive control but not for FUBL-1::3xFLAG or wild type (Figure1(B), indicating that the strains had been mixed up.

Genotyping wild type and FUBL-1::3xFLAG strains

To confirm the mix up of strains, wild type and *fubl-1*::3xFLAG worms genotyped with FLAG flanking sequence specific primers (described in appendix) was used. As expected from the Western blots, both strains were wild type for *fubl-1* (Figure 2(A), Next, wild type and *fubl-1*::3xFLAG strains were thawed fresh from the freezer stock, grown and genotyped. A band of expected size was observed in the fresh *fubl-1*::3xFLAG strain in comparison to wild type (Figure (B) and this strain was used for further experiments.

***fubl-1* isoform a disruption shows a similar phenotype to all isoforms disruption**

The effect of 3x FLAG tag in *fubl-1*::3xFLAG was investigated with RT-qPCR. Analysis of RT-qPCR results showed a similar expression of both tested ERGO-1 target genes in wild type and *fubl-1*::3xFLAG (p-value: 0,596 for *E01G4.5, p-value:* 0,845 for *E01G4.7*(A). This indicates that the FLAG tag does not affect FUBL-1 function.

The Hinas lab has investigated the role of FUBL-1 in endogenous 26G RNA pathway in two developmental stages (L4 and gravid adult). RT-qPCR was performed with ERGO-1 targets in wild type and a *fubl-1* Δ mutant. Results showed an upregulation in ERGO-1 target mRNA relative expression in the *fubl-1* Δ strain in comparison to wild type (Roy et al., manuscript in preparation).

To understand the role of *fubl-1* isoform A, ERGO-1 targets mRNA expression was analysed with RT-qPCR in wild type, *fubl-1 Δ*, *fubl-1 iso a (-)*, and disruption of all isoforms in *fubl-1 iso a+c (-)*. *E01G4.5* and *E01G4.7* mRNA expression was upregulated in *fubl-1 Δ*, *fubl-1 iso a (-)*, and *fubl-1 iso a+c (-)*.

FUBL-1 A importance was investigated by comparing gene expression in *fubl-1 iso a (-)* to *fubl-1 Δ*. There was no statistically significant difference between *fubl-1 Δ* and *fubl-1 iso a (-)* in *E01G4.5* (n=2, p-value: 0.07). However, the low number of biological replicates probably contributed to this and that it should be repeated with more replicates. We know that FUBL-1 is needed to regulate the expression of ERGO-1 targets *E01G4.5* and *E01G4.7*. Based on RT-qPCR results we suggest that the nonsense mutation affecting all predicted isoforms (isoform a+c (-)) shows similar upregulation as deletion as expected.

The importance of FUBL-1-A is still not fully understood although the results present a hint that FUBL-1-A might have an important role, but more investigation is needed to confirm it.

Optimization of *C. elegans* growth using *E. coli* strain NA22

Worms in this study were cultured at NGM plates seeded with *E. coli* strain OP50 in 10 cm plates which can fit maximum around 3000 eggs. Worms in this study should not be triggered by any stress (including starvation) as FUBL-1 might act differently to adapt to stress. That is why optimization was needed to grow non starved large, synchronized population.

To be able to perform RNA-immunoprecipitation, at least 100,000 gravid adult *C. elegans* were needed per strain (Tyc *et al.* 2017). Multiple research papers have used E. coli NA22 strain to grow large, synchronized *C. elegans* populations (Evans, 2006). As we did not know how many worms can grow on one large plate seeded with NA22 (Evans, 2006), I set up an experiment to test this (outlined in Figure (A). Wild type worms were grown, treated with bleach solution to prepare eggs and different number of eggs (2000, 3000, 4800,16000) were distributed on peptone rich media seeded with NA22 (Evans, 2006). In parallel, 3000 eggs were plated on NGM media seeded with OP50 (Brenner, 1974) plate. Worms were checked daily, After 3 days, worms on plates seeded with OP50 (Brenner, 1974) developed into

gravid adults however they were almost starved, in contrast to worms on plates seeded with NA22 (Evans, 2006) which were L3/L4 stage. On the fourth day, the plates seeded with NA22 (Evans, 2006), were checked, 16000 worms grew into gravid adult, and they were not starved. I found out that worms fed with NA22 (Evans, 2006), develop slower in comparison to worms fed with OP50 (Brenner, 1974).This was an important optimization for the continuation of the project.

FUBL-1::FLAG immunoprecipitation

The pilot RNA-immunoprecipitation (IP) experiment was performed with wild type and *fubl-1*::3xFLAG strains using anti-FLAG antibody-coupled magnetic beads. I first assessed whether FUBL-1::3xFLAG had been immunoprecipitated by analysing Input and IP protein preparations for each strain. All four samples were loaded twice on the same SDS-PAGE gel. Half of the gel was used for Western blot analysis using anti-FLAG antibody and the other half for Coomassie staining of total protein (Figure (A). For the Western blot, two bands around 70 kDa were observed in FUBL-1::FLAG IP eluate. These are suspected to be isoforms a and c but further investigation is needed to confirm this. In addition, a smaller band around 55 kDa is observed in both IP eluate and input which is suspected to be 2-Mercapto ethanol artifact. No bands were observed in WT input and IP, indicating that the IP was specific for FUBL-1::3xFLAG. Loading less than 10% of IP eluate and running the gel for a longer time might be needed in future to have better separation. Three bands around 130 kDa in FUBL-1 but not in input are likely IP-associated artifacts as they are not visible in the input sample.

The Coomassie staining showed that very little protein was detected after IP, indicating that the IP was specific for FUBL-1::3xFLAG (Figure 5(B).

FUBL-1::3xFLAG bound mRNA was successfully eluted

Protein analysis has showed that FUBL-1::3xFLAG was specifically immunoprecipitated. To assess whether it binds to RNA, RT-qPCR was performed.

Due to the lack of time, sequencing was not an option to determine FUBL-1 bound RNA, but the efficiency of mRNA elution was tested by RT-qPCR (Figure 0. Based on figure 0 FUBL-1::3xFLAG bound mRNA was successfully eluted.

Discussion

In recent years, it has been established that in addition to genetic information, non-genetic information can be transmitted to the progeny (Lacal & Ventura 2018). This phenomena have been documented in different organisms including animals (Skvortsova *et al.* 2018). However, the mechanisms of epigenetics inheritance through DNA methylation, histone modification, and non-coding RNAs are still an enigma to solve (Skvortsova *et al.* 2018).

The human far upstream binding protein 1 (FUBP1) and far upstream binding protein 3 (FUBP3) ortholog of FUBL-1 in *C. elegans* have been identified as single stranded DNA and RNA binding proteins (Wormbase. https://wormbase.org, Zhang & Chen 2013). Multiple studies identified FUBP1 as *c-Myc* proto-oncogene transcription regulator (Zhang & Chen 2013). To explain further, FUBP1 upregulates *c-Myc* expression by binding to the far upstream element (FUSE), located upstream *c-Myc* promoter transcription site, to promote transcription factor II H (TFIIH) helicase activity and *c-Myc* transcription (Zhang & Chen 2013). FUBP1 knockdown in human hepatocellular carcinoma (HCC) cell lines reduces *c-Myc* expression, cell proliferation, and tumor formation in mouse xenograft models (Rabenhorst *et al.* 2009). Furthermore, FUBP1 knockout might result in mice death at embryonic day 10.5 or after birth (Zhou *et al.* 2016). However, FUBP1 activity can be hindered by FUBP interacting repressor (FIR), thus blocking FUBP1-dependent *c-Myc* transcription to control *c-Myc* expression level (Zaytseva & Quinn 2017). The study of Zhang and colleagues (2020) showed that chromatin architecture is altered in FUBP1 knock out (KO) and knockdown (KD) cells. The Chip-PCR and nuclease hypersensitivity experiments suggested that FUBPs enforce epigenetic modifications which in turn influences *c-Myc* expression (Zheng *et al.* 2020).

Recent evidence indicated that FUBP is a master regulator of transcription, mRNA degradation, splicing, translation, and has a prominent role in carcinogenesis (Zhang & Chen 2013). However, the role of FUBPs in epigenetic regulation is still not clear (Zheng *et al.* 2020).

In this study, I investigated the role of FUBL-1 isoforms in the ERGO-1 pathway. I showed that there was, as expected, similar upregulation of ERGO-1 targets' gene expression in the mutant carrying a nonsense mutation disrupting all isoforms (*fubl-1 isoform a+c (-))* and in

the deletion mutant (*fubl-1 Δ*). Thus, we suggest that FUBL-1a and FUBL-1c might be the two dominant isoforms of *fubl-1* in the ERGO-1 pathway. However, it is interesting to investigate how FUBL-1 isoforms regulate ERGO-1 targets' expression and if the FUBL-1 isoforms function in a partnership, competition, or compensation pathway. Studies in the human FUBP showed an interplay between FUBP isoforms' functions in different pathways. For instance, FUBP1 and FUBP3 cooperate to promote EV71 replication while FUBP2 represses EV71 viral translation (Zheng *et al.* 2020).

Furthermore, I showed that statistically there was no significant difference between ERGO-1 targets' gene regulation in the *fubl-1 isoform a* disruption strain (*fubl-1 iso a (-)*), and all isoforms disruption strain (*fubl-1 Δ)*. This result suggests that FUBL-1a might not dominate ERGO-1 targets' regulation ((A).

It is still not understood how target transcripts are selected by 26G RNAs, but it was suggested by Newman and colleagues (2018) that RNAi targets in *C. elegans* are poorly conserved with few introns. This hypothesis was supported by biochemical evidence in which RNAi target transcripts were tightly bound to spliceosomes, suggesting that slow or inefficient splicing license the transcript for silencing in the endogenous RNAi pathway. Another study by Makeyeva and colleagues (2021), suggest that unspliced transcripts or intronless genes in the germline are silenced in *C. elegans* by RNAi dependent and independent pathways. Although more investigation is needed, Makeyeva and colleagues (2021) hypothesize that cues from splicing protect or license the transcript for silencing by the RNAi machinery in the germline.

Miro and colleagues (2015) study demonstrate through RNA pull down and RNA EMSA experiments that FUBP1 is bound to pre-mRNA in the intronic splicing enhancer (ISE) element. This was confirmed by RNA-Chip on endogenous *Duchenne muscular dystrophy* (*DMD*) pre-mRNA. Other studies supported the involvement of FUBP1 in splicing but its role in splicing and target RNAs are still unknown.

Moreover, I investigated the functionality of FUBL-1::3xFLAG strain and demonstrated that the C-terminal 3x FLAG tag in FUBL-1 constructed by the Hinas group did not affect FUBL-

1 function as this strain showed a similar ERGO-1 target gene expression as the wild type by RT-qPCR ((A). This finding was crucial to carry out the pilot IP experiment.
The western blot experiment demonstrated that FUBL-1::3xFLAG protein was successfully immunoprecipitated (Figure 5**: FUBL-1::3xFLAG immunoprecipitation**). In addition, FUBL-1::3xFLAG bound mRNAs was successfully eluted according to RT-qPCR (Figure 6: **FUBL-1::3xFLAG bound mRNA was successfully eluted**. A potential optimization of this method can be by assessing eluted RNA concentration and quality with Qubit.

Multiple studies have confirmed that RNA binding proteins (RBP) with K homology (KH) domain bind to small RNAs and regulate gene silencing (Haskell & Zinovyeva 2021). Haskell and Zinvyeva (2021) showed through knocking down KH domain encoding genes in *C. elegans* that RBP with the KH domain interacts with several miRNAs. The result suggested that RBP with KH domain interact with miRNAs directly through affecting their biogenesis, or indirectly through affecting miRNA's target mRNA biogenesis to regulate gene expression post-transcriptionally. Haskell and Zinovyeva (2021) RNAi experiments suggest that FUBL-1 interacts with mir-48, mir-241 and let-7. In line with this we suggest that FUBL-1 binds to mRNA (0 and might interact with small RNAs.

At present we do not know to which RNAs, and proteins FUBL-1 is bound, and how it acts in the endogenous 26G RNAi pathway. However, we know that it acts in the ERGO-1 pathway and FUBL-1 isoforms function should be further investigated. Although more investigation is needed, we suggest that FUBL-1a might have a role downstream in the 26G pathway and might bind to 22G when it is transported to the nucleus as it has a nuclear localisation signal.

The optimization of growing a large, synchronized *C. elegans* population and RNA-IP pilot study will be instrumental for the continuation of the project. Future work could include identifying FUBL-1 bound RNAs by sequencing and FUBL-1 bound proteins by co-IP and mass spectrometry.

Acknowledgment

I would like to thank my supervisor Andrea Hinas for her guidance, support and for motivating and pushing me during my thesis and Shweta Roy for her help and guidance. The worm lab members: Martin Lind, Claudia Aldeia, Gieorgia Fiorino, and Joel Pålsson and my coordinator David van der Spoel.

Moreover, I would like to thank the Micro group family for their friendly and cooperative lab atmosphere. Bart Edelbroek for his suggestions and help in the immunoprecipitation experiment, Thomas Stenum for kindly providing me with the antibodies, and Margareta Komi for her friendship and support.

I am grateful for my friends in Uppsala who made this journey unforgettable and with whom I shared my ups and downs and many laughs, my very first friend Huzaifah, my amazing corridor friend and sister Laura Chan, my lovely "Saturday people" Sibel Özcan, Özlem Dilaver, Nader Talaat, and Sara Magnusson and my "Chopinitos" Alejandra Pazmiño, Alex Perez, Leire, and Lucia Sancho. Also, for the Benwermarna- Värmlands dansgrupp big family and my "salsa and Bachata friends" Ella, Lefteris, Tong, Christine, Tej, and Jordi, and My khlg Family and specially the amazing Letta Gardet. Finally, my family for their love and continuous support.

References

Almeida, M. V., Andrade-Navarro, M. A. and Ketting, R. F. (2019) Function and evolution of nematode RNAi pathways, *Non-coding RNA*.

Corsi AK, Wightman B, Chalfie M. 2015. A Transparent Window into Biology: A Primer on Caenorhabditis elegans. Genetics 200: 387–407.

Evans TC. 2006. Transformation and microinjection. WormBook

fubl-1 (gene) - WormBase : Nematode Information Resource. online: https://wormbase.org/species/c_elegans/gene/WBGene00007534#0-9f-10. Accessed May 23, 2022.

Fire, A. *et al.* (1998) Potent and specific genetic interference by double-stranded RNA in Caenorhabditis elegans, *Nature*, 391(6669),806–811.

Grishok A. 2005. RNAi mechanisms in Caenorhabditis elegans. FEBS Letters 579: 5932–5939.

Haskell D, Zinovyeva A. 2021. KH domain containing RNA-binding proteins coordinate with microRNAs to regulate Caenorhabditis elegans development. G3 Genes|Genomes|Genetics 11: jkab013.

Heijmans BT, Tobi EW, Stein AD, Putter H, Blauw GJ, Susser ES, Slagboom PE, Lumey LH. 2008. Persistent epigenetic differences associated with prenatal exposure to famine in humans. Proceedings of the National Academy of Sciences of the United States of America 105: 17046–17049.

Kappeler L, Meaney MJ. 2010. Epigenetics and parental effects. BioEssays 32: 818–827.

Kelly, W. G. *et al.* (1997) 'Distinct requirements for somatic and germline expression of a generally expressed Caenorhabditis elegans gene', *Genetics*, 146(1),227–238.

Kim J, Gabel H, Kamath R, Tewari M, Pasquinelli A, Rual J-F, Kennedy S, Dybbs M, Bertin N, Kaplan J, Vidal M, Ruvkun G. 2005. Functional Genomic Analysis of RNA Interference in C. elegans. Science (New York, NY) 308: 1164–7.

Lacal I, Ventura R. 2018. Epigenetic Inheritance: Concepts, Mechanisms and Perspectives. Frontiers in Molecular Neuroscience 11:

Li, S. *et al.* (2004) A map of the interactome network of the metazoan C. elegans., *Science (New York, N.Y.)*, 303(5657),540–3.

Makeyeva YV, Shirayama M, Mello CC. 2021. Cues from mRNA splicing prevent default Argonaute silencing in C. elegans. Developmental Cell 56: 2636-2648.e4.

Miro J, Laaref AM, Rofidal V, Lagrafeuille R, Hem S, Thorel D, Méchin D, Mamchaoui K, Mouly V, Claustres M, Tuffery-Giraud S. 2015. FUBP1: a new protagonist in splicing regulation of the DMD gene. Nucleic Acids Research 43: 2378–2389.

Newman MA, Ji F, Fischer SEJ, Anselmo A, Sadreyev RI, Ruvkun G. 2018. The surveillance of pre-mRNA splicing is an early step in C. elegans RNAi of endogenous genes. Genes & Development 32: 670–681.

Rabenhorst U, Beinoraviciute-Kellner R, Brezniceanu M-L, Joos S, Devens F, Lichter P, Rieker RJ, Trojan J, Chung H-J, Levens DL, Zörnig M. 2009. Overexpression of the far upstream element binding protein 1 in hepatocellular carcinoma is required for tumor growth. Hepatology (Baltimore, Md) 50: 1121–1129.

Shen L, Li C, Wang Z, Zhang R, Shen Y, Miles T, Wei J, Zou Z. 2019. Early-life exposure to severe famine is associated with higher methylation level in the IGF2 gene and higher total cholesterol in late adulthood: the Genomic Research of the Chinese Famine (GRECF) study. Clinical Epigenetics 11: 88.

Skvortsova K, Iovino N, Bogdanović O. 2018. Functions and mechanisms of epigenetic inheritance in animals. Nature Reviews Molecular Cell Biology 19: 774–790.

Theil K, Imami K, Rajewsky N. 2019. Identification of proteins and miRNAs that specifically bind an mRNA in vivo. Nature Communications 10: 4205.

Tyc KM, Nabih A, Wu MZ, Wedeles CJ, Sobotka JA, Claycomb JM. 2017. The Conserved Intron Binding Protein EMB-4 Plays Differential Roles in Germline Small RNA Pathways of C. elegans. Developmental Cell 42: 256-270.e6.

Vågerö D, Pinger PR, Aronsson V, van den Berg GJ. 2018. Paternal grandfather's access to food predicts all-cause and cancer mortality in grandsons. Nature Communications 9: 5124.

Wu, E. *et al.* (2017) A continuum of mRNP complexes in embryonic microRNA-mediated silencing, *Nucleic Acids Research* 45(4):2081-2098.

Yuan JS, Reed A, Chen F, Stewart CN. 2006. Statistical analysis of real-time PCR data. BMC Bioinformatics 7: 85.

Zaytseva O, Quinn LM. 2017. Controlling the Master: Chromatin Dynamics at the MYC Promoter Integrate Developmental Signaling. Genes 8: 118.

Zhang J, Chen Q. 2013. Far upstream element binding protein 1: a commander of transcription, translation and beyond. Oncogene 32: 2907–2916.

Zheng Y, Dubois W, Benham C, Batchelor E, Levens D. 2020. FUBP1 and FUBP2 enforce distinct epigenetic setpoints for MYC expression in primary single murine cells. Communications Biology 3: 1–11.

Zhou W, Chung YJ, Parrilla Castellar ER, Zheng Y, Chung H-J, Bandle R, Liu J, Tessarollo L, Batchelor E, Aplan PD, Levens D. 2016. Far Upstream Element Binding Protein Plays a Crucial Role in Embryonic Development, Hematopoiesis, and Stabilizing Myc Expression Levels. The American Journal of Pathology 186: 701–715.

Appendix

Table S1: Primer list

Oligo name	Sequence	
301_eif-3.c_fwd	ACACTTGACGAGCCCACCGAC	endogenous reference gene pimers
302_eif-3.c_rev	TGCCGCTCGTTCCTTCCTGG	endogenous reference gene pimers
331_FUBL-1::FLAG F	CGGTTGTACCAGGTGGACTC	confirmation of FUBL:3X FLAG
332_FUBL-1::FLAG R	CCTTGGCGGCAAATGATGTC	confirmation of FUBL:3X FLAG
315_E01G4.5 F	CTCAAGAAAGTTTCACAGCAGGCC	ERGO1 pathway genes
316_E01G4.5 R	CACTTACACAAAACATTTCTC	ERGO1 pathway genes
307_E01G4.7 F	GCACAAGGTTTCGTTCTTGGTG	ERGO1 pathway genes
308_E01G4.7 R	AGTGACATCCCTTCTGATCG	ERGO1 pathway genes